Journal of Biomedical Optics

BiomedicalOptics.SPIEDigitalLibrary.org

Study of the inhibition effect of thiazone on muscle optical clearing

Xiaowei Jin
Zhichao Deng
Jin Wang
Qing Ye
Jianchun Mei
Wenyuan Zhou
Chunping Zhang
Jianguo Tian

SPIE.

Xiaowei Jin, Zhichao Deng, Jin Wang, Qing Ye, Jianchun Mei, Wenyuan Zhou, Chunping Zhang, Jianguo Tian, "Study of the inhibition effect of thiazone on muscle optical clearing," *J. Biomed. Opt.* **21**(10), 105004 (2016), doi: 10.1117/1.JBO.21.10.105004.

Study of the inhibition effect of thiazone on muscle optical clearing

Xiaowei Jin,[a,b] Zhichao Deng,[a,b] Jin Wang,[a,b] Qing Ye,[a,b,*] Jianchun Mei,[b,c] Wenyuan Zhou,[a,b] Chunping Zhang,[a,b] and Jianguo Tian[a,b]
[a]Nankai University, School of Physics and TEDA Applied Physics School, Key Laboratory of Weak-Light Nonlinear Photonics, Ministry of Education, 94th Weijin Road, Tianjin 300071, China
[b]Nankai University, The 2011 Project Collaborative Innovation Center for Biological Therapy, 94th Weijin Road, Tianjin 300071, China
[c]Nankai University, Advanced Technology Institute, 94th Weijin Road, Tianjin 300071, China

Abstract. We investigated the effect of thiazone, a widely used penetration enhancer, on *in vitro* porcine skin and muscle tissue by single-integrating sphere technique during optical clearing (OC) treatment. The results showed that thiazone induced an increase on the total transmittance of skin which led to a reduction in that of muscle in the spectral range from 400 to 800 nm. Small particles crystalized out from the thiazone-treated muscle were observed by microscopy imaging. With the help of x-ray diffraction measurement, we ascertained that the crystal was a single-crystal of thiazone, which mainly induced an increase of the scattering. Contrast transmittance measurements carried on the mixture of water, thizaone–propylene glycol solution showed that the free water in muscle could be the main reason for the thiazone crystallization. Therefore, during OC treatment of thiazone, the remarkable effect on skin and the noticeable inhibition effect on subcutaneous muscle tissue after penetrating into the skin should be considered. The experimental results provide such a reference for the choice of penetration enhancer. [DOI: 10.1117/1.JBO.21.10.105004]

Keywords: thiazone; optical clearing; inhibition; single-integrating sphere; skin; muscle.

Paper 160303RRR received May 13, 2016; accepted for publication Sep. 28, 2016; published online Oct. 20, 2016.

1 Introduction

Nowadays, biomedical photonics plays a significant role in the research of optical diagnosis, biomedical imaging, laser therapy, and so on. The constituents of biotissue not only include low-refractive-index (RI) interstitial fluid and cytoplasm,[1] but also some high-RI components, such as cell membrane, cell nucleus, organelles, and melanin. The RI mismatch between high-RI and low-RI components that limit the penetration depth of light in tissue[2,3] is the origin of tissue scattering. The optical clearing (OC) technique proposed by Tuchin et al.[4] is an effective method to reduce the RI mismatches with a high-RI agent, which is commonly designed as an optical clearing agent (OCA). An OCA must meet the need of being a nontoxic for producing no side effects when it is applied on the biotissues. Glycerol,[5–8] polyethylene glycol 400 (PEG400),[9] glucose,[10–14] propylene glycol,[15–17] and others have often been used in OC treatments of different biological tissues [3–8] and other tissues, such as skull and cartilage, and so on.[18–20] OC begins with OCA application to the tissues. OCAs usually create a transparency effect on tissues by the combination of some reported mechanisms such as the dehydration mechanism,[17,21] the refractive index matching mechanism,[3,7,10,13,22–27] and in some cases collagen solubility.[13,28–31] Meanwhile, to detect the efficiency of OCAs on OC treated tissue, the integrating sphere technique,[9,32–36] the derivative total reflection method,[37–40] the resolution target imaging,[41] CCD microimaging,[42] and optical coherence tomography (OCT) [15,43,44] have been proposed.

Stratum corneum (SC), the outermost layer of the epidermis, is the main component that hinders OCAs from infiltrating into the skin. To weaken the inhibition of skin, some chemical agents that can either modify the SC's structure reversibly or reinforce the fluidity of SC are applied on the surface of skin, such as azone,[33,45] thiazone,[33,43,44,46] oleic acid,[47,48] and dimethyl sulfoxide (DMSO).[49–52] Thiazone, one of the derivatives of azone, has been reported as an effective permeation enhancer to the OC treatment of skin. The infiltration capacity of thiazone is nearly 2.99 times higher than that of azone.[53] It was reported that the efficiency of OC on human dorsal hand skin increased roughly 33.33% when treated with 0.25% thiazone PEG400 solution.[44]

Numerous studies have been done to promote the skin's OC while decreasing the limit of SC. However, the SC thickness varies from 10 to 40 μm,[54] even though the epidermis thickness is nearly 0.1 mm.[55,56] It has been indicated that the $Z_{\text{threshold}}$, the depth at which the OCT signal dropped below a threshold signal of 10^{-5} reflectance, increased from 0.219 to 0.275 mm for rat skin during a 15-min application of 5% thiazone-PEG400,[43] and the shallow $1/e$ light penetration depth that was detected by OCT increased from 0.35 to 0.47 ± 0.02 mm for human skin during a 60-min treatment of 0.25% thiazone-PEG400.[44] This reveals that thiazone mixed with OCAs can easily enhance diffusion through the skin and quickly have an effect on the subcutaneous muscle tissue. Although several reports have discussed the impact of OC on muscle treated with different OCAs,[7,11,13,23–25,39,40] an understanding of the influence of the clearing on muscle exposed to permeation enhancers, such as thiazone and azone, has remained incomplete.

In this study, we use the integrating sphere technique and a CCD microimaging system to investigate the OC efficiency of different concentrations of thiazone–propylene glycol solution

*Address all correspondence to: Qing Ye, E-mail: yeqing@nankai.edu.cn

1083-3668/2016/$25.00 © 2016 SPIE

on *in vitro* porcine muscle and skin, respectively. The efficiency of OC on skin fits well with previous studies,[44–46] whereas the result on muscle is quite different from others.[11] We discover that thiazone induced decrease of OC efficiency on muscle tissue and the remarkable inhibition effect of 10% thiazone–propylene glycol solution.

2 Materials and Methods

2.1 *Materials*

Fresh *in vitro* griskin with less fat and porcine skin on the back was chosen from an accredited abattoir with no visible scratches or abrasions. Samples were preserved at −3 to 0°C to remain fresh during the 1-h transportation. Before experiments, the muscle was sealed and frozen for nearly 5 h. Meanwhile, the hog hair and fat of the skin was carefully removed and washed by phosphate buffered saline (PBS) to remove impurities on the surface. Then the muscle and skin samples were cut into small pieces (3×3 cm^2) with a thickness of ~2 and 2.12 ± 0.26 mm, respectively. Samples were wrapped with cling film to prevent the natural dehydration and were thawed to room temperature.

2.2 *Thiazone and Propylene Glycol Treatment*

Thizone (Gao Jin Medicine, Henan, China), a nonirritating penetration enhancer, is a white or flaxen crystal at room temperature with a melting temperature ranging from 30 to 40°C. Propylene glycol (PG) (Kermel, Tianjin, China), one of common and effective OCAs for biotissue, is widely applied on the OC treatment of skin and can mix with water at different ratios.

Thiazone was melted at 40°C prior to experiments, and then mixed with PG at different proportions. The solutions were sealed at room temperature. Experiments were performed in five situations as presented in Table 1.

2.3 *Spectral Measurement*

A schematic diagram of the total transmittance measurement system is shown in Fig. 1. The sample was held between two slides of glass and then fixed by a plastic holder with a circle window. White light from a xenon lamp was transported through an aperture A before arriving the converging lens L. Collimated light coming out from L was divided into two parts after being transported through a splitter M. One part irradiated the detector D as the monitor and the other illuminated the sample. The transmittance was collected by a single integrating sphere and a spectrometer (Ocean Optics HR4000). Different agents and similar processes were applied on one side of the muscle and the epithelial surface of the skin. The residual agents on the surface of the sample were removed before measurements. Light was illuminated from the side that has been applied by agents.

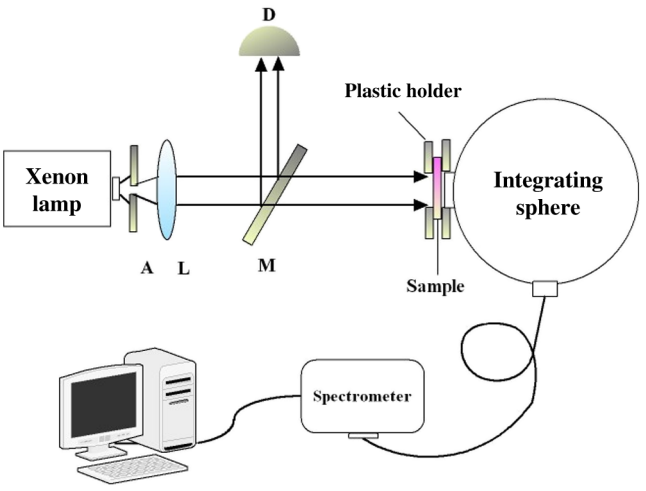

Fig. 1 Schematic diagram of the total transmittance measurement system.

The tendency of the OC effect could be qualitatively evaluated from the total transmittance spectra, yet the quantitative information could not be obtained. We defined the increment of total transmittance (ΔT) at 563.5 nm to quantitatively calculate the transmittance. Total transmittance spectra were taken at a time interval of 5, 10, 15, 20, 30, 40 min, respectively. Each experiment was measured three times. The expression of ΔT with different time intervals was given by[44]

$$\Delta T = \frac{T_x - T_0}{T_0} \times 100\%, \tag{1}$$

where T_0 and T_x are the measured total transmittances at 563.5 nm for each group at the time intervals of 0 and x min, respectively.

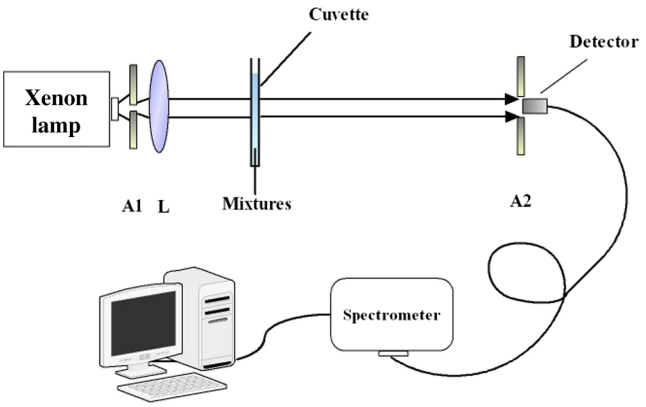

Fig. 2 Schematic diagram of the collimated transmittance measurement system.

Table 1 Agents in our study.

Groups	Control	PG	1%T/PG	3%T/PG	10%T/PG
Solutions	—	Propylene glycol	Propylene glycol with 1% thiazone	Propylene glycol with 3% thiazone	Propylene glycol with 10% thiazone

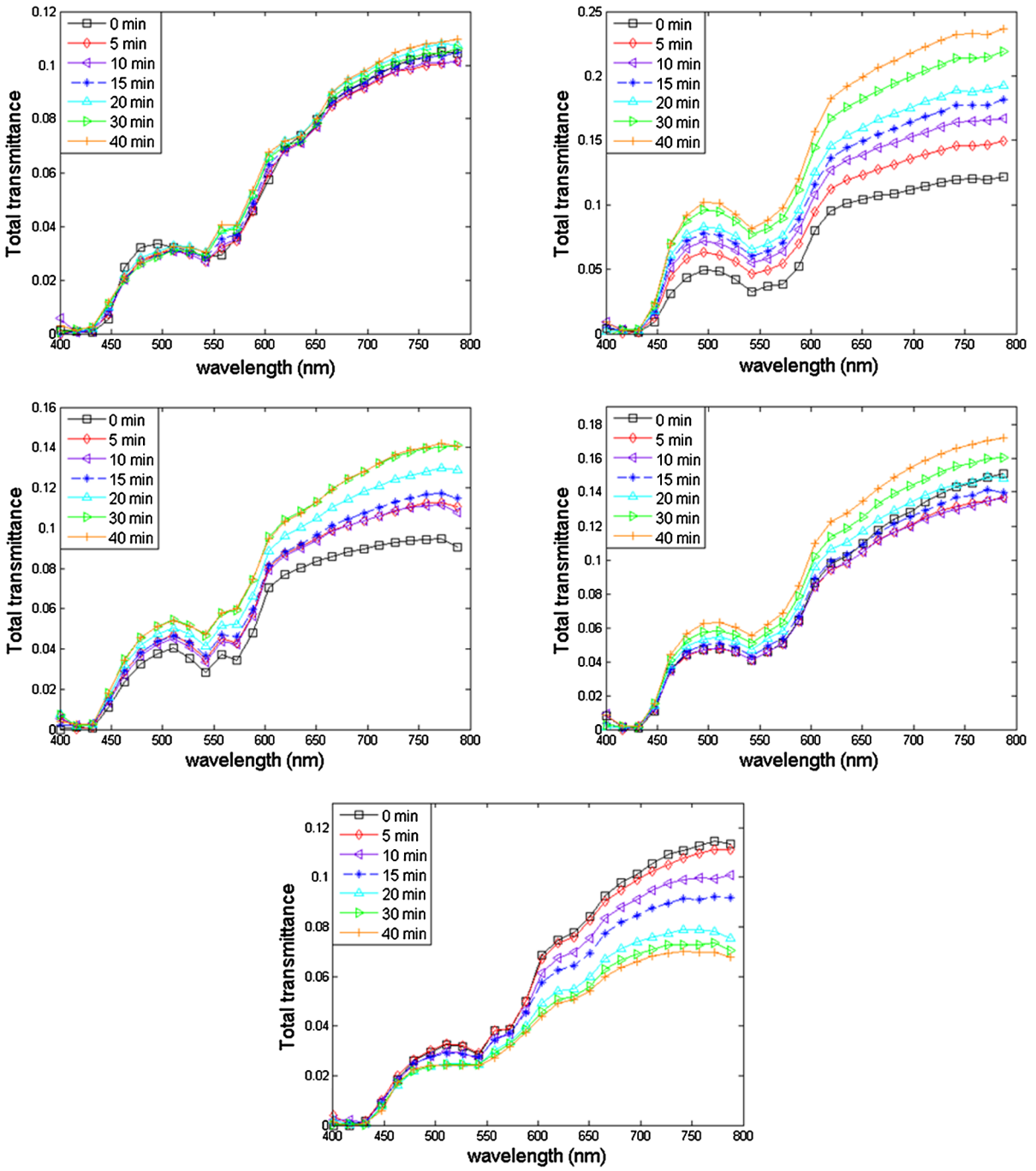

Fig. 3 Total transmittance spectra of fresh *in vitro* porcine muscle at a time interval of 5, 10, 15, 20, 30, and 40 min relative to (a) control group, (b) PG group (b), (c) 1%T/PG group, (d) 3%T/PG group, and (e) 10%T/PG group.

2.4 *CCD Microimaging System*

We utilized a CCD microimaging system to detect the structure changes both outside and inside of the sample for two different thickness samples (2 and 1 mm) after applying thiazone-PG solution. Sample A (1 mm) was covered on sample B (2 mm), and PG and 3% thiazone PG solution were then only applied on the surface of sample A, respectively. The remaining agents were removed after 40 min. Sample A and sample B were placed between two glass slides, respectively, and positioned on the microscope stage of an inverted microscope (SW-1000). The microimages were acquired by the CCD microimaging system.

2.5 *Collimated Transmittance Measurement*

PG, 1%T/PG, 3%T/PG solutions were mixed with water at a ratio of 1:9, respectively, and experiments were divided into four groups: water, PG/W, 1%T/PG/W, and 3%T/PG/W. Mixtures were injected into a cuvette with a thickness of 1 mm. The schematic diagram of the collimated transmittance measurement system is shown in Fig. 2. White light from a xenon lamp was transported through an aperture A1 before arriving to the converging lens L. Collimated light coming out from L illuminated the cuvette (1 mm). The collimated transmittance was collected by a spectrometer (Ocean Optics

HR4000) behind another aperture A2. The total attenuation coefficient was calculated using the Lambert–Beer law.

3 Results

3.1 *Measured Total Transmittance Spectra*

3.1.1 *In vitro porcine muscle*

The transmittance spectra of samples treated with different solutions were measured by an integrating sphere and presented in Fig. 3.

Due to the natural dehydration, a slight increment appears on the total transmittance of the control group [Fig. 3(a)]. In comparison with the control group, the total transmittance with PG treated increases absolutely during 40 min [Fig. 3(b)]. Interestingly, as illustrated in Fig. 3(c), the total transmittance of the 1%T/PG group at 5 min induces a similar increase compared with that of 1%T/PG group at 10 min. Meanwhile, the total transmittance of 3%T/PG group decreases at a time interval of 5 min [Fig. 3(d)]. For the sample treated with 10%T/PG, total transmittance reduces after agent treatment [Figs. 3(e) and 4], and an obvious decrease can be observed with a longer treatment.

To quantitatively analyze the effect of thiazone on the OC of fresh *in vitro* porcine muscle, ΔT is evaluated by Eq. (1) and the results are shown in Fig. 4.

Statistics reveal that, compared with the control group, the ΔT of PG group increases about 4 times after a 40-min treatment. Yet, in contrast with PG group, there is no such huge increase in the ΔT of the 1%T/PG and 3%T/PG groups. The values of ΔT in response to the PG, 1%T/PG, and 3%T/PG groups within a 40-min increase from 32.48%, 21.03%, and 0.58% to 127.24%, 57.12%, and 36.00%, respectively. The increasing rates of ΔT of PG, 1%T/PG, and 3%T/PG groups are 2.71%, 1.03%, and 1.01% per min, respectively. Obviously, the thiazone-treated groups have a lower increase rate of ΔT. In the case of 10%T/PG group, ΔT drops to −0.07% within the first 5 min, and shows a continually negative increase all the way between 10 and 40 min. It reveals that thiazone inhibits the OC efficiency of PG and increases the scattering of muscle. The 10%T/PG group induces the largest increase of scattering, whereas the 1%T/PG group induces the lowest. The experimental results support the inhibition effect of thiazone on OCA treatment of muscle, what is more, the extent of inhibition increases with the concentration of thiazone.

During the experiments of the 1%T/PG group, 3%T/PG group, and 10%T/PG group, we discovered that some white crystals emerged in muscle when agents were applied and the amount of crystals aggrandized with the increase of concentration of thiazone. To analyze the components of these crystals, CCD microimaging and x-ray single crystal diffractometer were preformed, which will be discussed later.

3.1.2 *In vitro porcine skin*

To compare the OC effect of thiazone for muscle and skin, we measured the increment of total transmittance on *in vitro* porcine skin at 563.5 nm.

As shown in Fig. 5, for all chemical agent groups, ΔT increases much faster than that of the control group. Statistics show that the PG group, 1%T/PG group, 3%T/PG group, and 10%T/PG group induce 14.66%, 18.96%, 21.30%, and 26.59% increases in ΔT at 5 min, respectively, whereas only a 3.02% change was observed in the control group. Meanwhile, similar increases in OC were obtained for the 10%T/PG group past 5 min and control group past 30 min. This indicates that thiazone promotes the efficiency of OC on skin, and the efficiency of OC increases with the concentration of thiazone. The tendency of the OC effect on thiazone-treated skin agrees well with previous reports.[44,46] Compared with the effect of thiazone on OC or fresh porcine muscle, the effect on skin is quite different from that on muscle. Thiazone has no effect on the OC of muscle and even produces an inhibition effect at high concentrations, whereas it effectively promotes the OC efficiency of *in vitro* porcine skin. Hence, thiazone is not suitable for the OC treatment on muscle.

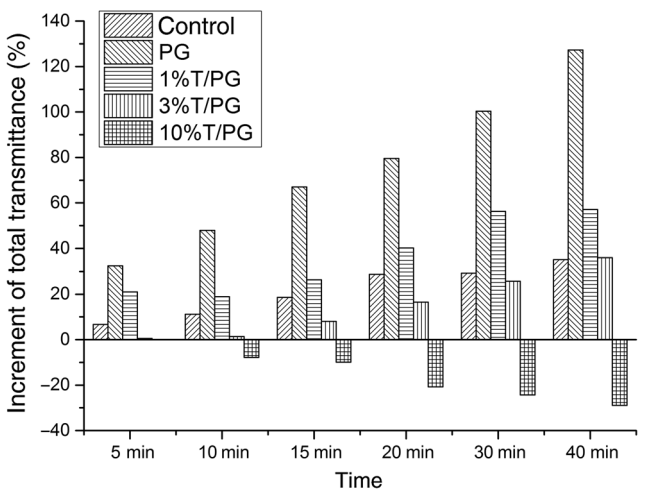

Fig. 4 Increment in total transmittance at 563.5 nm of fresh *in vitro* porcine muscle with the treatment of nothing, pure PG, 1%T/PG, 3%T/PG,10%T/PG, at a time interval of 5, 10, 15, 20, 30, and 40 min, respectively.

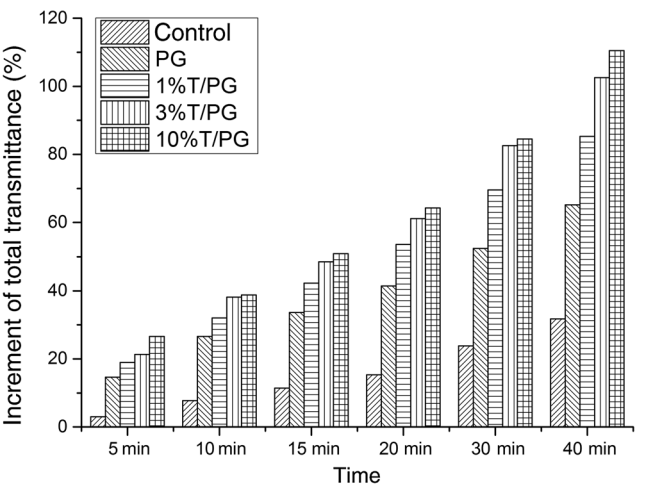

Fig. 5 Increment in total transmittance at 563.5 nm of fresh porcine skin *in vitro* with the treatment of nothing, pure PG, 1%T/PG, 3%T/PG, 10%T/PG, at a time interval of 5, 10, 15, 20, 30, and 40 min, respectively.

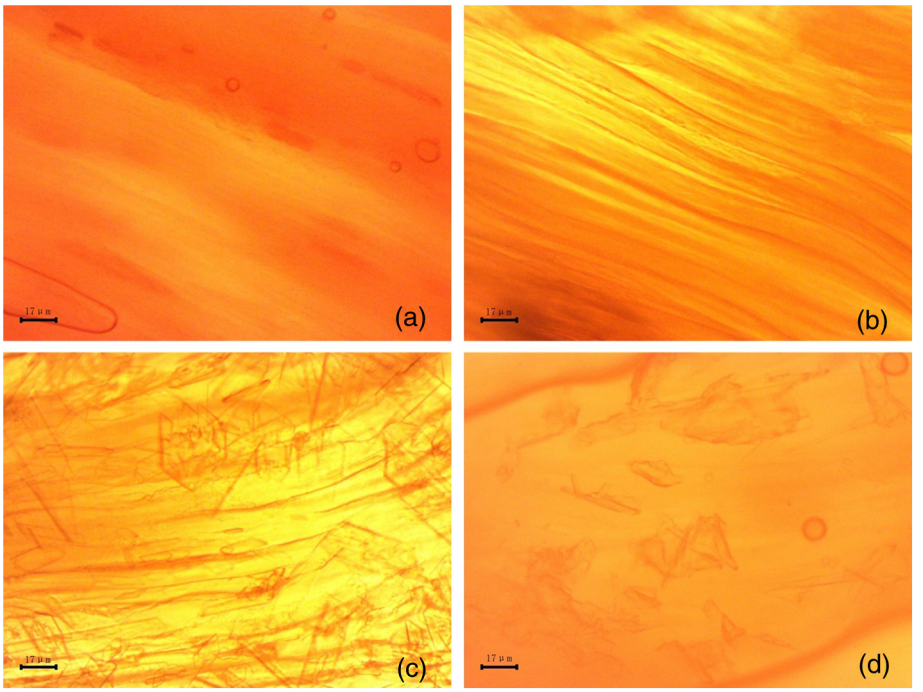

Fig. 6 The microimages of *in vitro* fresh porcine muscle by CCD camera at the time interval of 40 min. (a)–(d) Sample B of control group, sample B of PG group, sample A of 3%T/PG group, and sample B of 3%T/PG group, respectively.

3.2 *CCD Microimaging and X-Ray Single-Crystal Diffractometer*

Microimages of samples obtained by the CCD microimaging system at the time interval of 40 min are shown in Fig. 6, corresponding to (a) sample B of control group, (b) sample B of PG group, (c) sample A of 3%T/PG group, and (d) sample B of 3%T/PG group.

For sample B of the control group and that of the PG group, though no crystal has been found, sample B of the PG group has a greater transmittance than that of the control group. Compared with the result of PG group, large quantities of crystals were observed on the surface of both samples A and B with the treatment of 3%T/PG. Thus, it indicates that thiazone-PG can easily penetrate through a 1 mm sample and crystals appear on both the outside and the inside of the muscle, which largely increases the scattering of samples.

To determine the type of crystals, a small amount of crystals is extracted and analyzed by x-ray single-crystal diffractometer (Rigaku 007 Saturn 70). Chemical ingredients, unit cell dimensions (Table 2), the structure refinement, and bond lengths show that the crystal appearing in the muscle is the single crystal of thiazone.

3.3 *Calculation of the Total Attenuation Coefficient*

To further prove the critical role of water content of muscle on the crystallization of thiazone, we perform the collimated transmittance measurement (Fig. 2). The attenuation coefficient of each group over the range from 400 to 800 nm is calculated using Lambert–Beer law. As shown in Fig. 7, the PG/W group and water group induce similar values. Compared with the PG group, the 1%T/PG/W group and 3%T/PG/W group induce an obvious increase in the attenuation coefficient, respectively. Statistics indicate that the attenuation coefficients of the 1%T/PG/W group and 3%T/PG/W group are about 64.7 and 122.3 times greater than that of the water group, respectively. Otherwise, we found that water became turbid when mixed with thiazone PG solution during the experiments. This reveals that crystals of thiazone appear when the T/PG solution was mixed with water. The water content of muscle tissue is of fundamental importance for the extraction of thiazone, which mainly induces the increase of the attenuation coefficient of the mixture.

Table 2 Part of the report of crystals by x-ray single crystal diffractometer.

Formula	$C_{11}H_{13}NO_3S$
Formula weight	239.28
Wavelength	0.71073 A
Unit cell dimensions	$a = 7.107(4)$ A alpha $= 103.824(7)$ deg
	$b = 7.431(4)$ A beta $= 91.717(8)$ deg
	$c = 11.447(6)$ A gamma $= 108.655(9)$ deg
Volume	$552.4(5)$ A^3
Z, calculated density	2, 1.438 Mg/m^3
Absorption coefficient	0.284 mm^{-1}
F (000)	252
Crystal size	$0.20 \times 0.18 \times 0.12$ mm
Limiting indices	$-9 \le h \le 9$, $-9 \le k \le 9$, $-14 \le l \le 14$

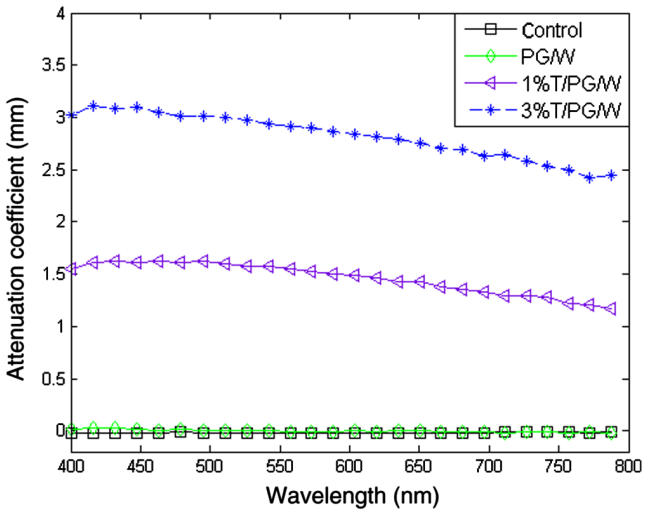

Fig. 7 The total attenuation coefficient of water group, PG/W group, 1%T/PG group, and 3%T/PG group.

4 Discussion

From analyzing the transmittance of fresh skin and muscle during the treatment with PG, we discover that PG can obviously reduce the scattering of muscle and skin. As shown in Fig. 5, the increment of total transmittance of skin treated with PG is nearly five times greater than that of the control group at a time interval of 5 min. This results from the hydrogen bonding between the hydrophilic hydroxyl of PG and water molecules in the muscle. Moreover, the dehydration effect of the PG group induces a much more effective penetration of agents into tissue and leads to a better RI matching environment. Our experimental results show that PG can effectively improve the effect of OC on both skin and muscle.

According to the results of the *in vitro* porcine skin experiment with different concentrations of thiazone-PG solution, the application of thiazone promotes the effect of PG on OC. On one hand, the usage of thiazone increases the fluidity of the lipid bilayer and improves the penetration of PG. On the other hand, PG that has been introduced into skin partly replaces the interstitial fluid and diminishes the RI mismatch in tissue. This suggests the synergistic effect of thiazone and PG. Our results agree well with Zhu's correlation between the thiazone PEG400 solution and the OC of fresh *in vitro* porcine skin.[46]

Yet, total transmittance spectrum of 10%T/PG group of muscle indicates that thiazone induces a decrease in OC on muscle [Fig. 3(e)]. Similarly, the CCD microimages show that large quantities of thiazone crystals are observed in muscle, which increase the scattering [Figs. 6(c) and 6(d)]. This is because of the different solubilities of thiazone and PG in water. Thiazone is unsoluable in water, yet PG can be mixed with water at any ratio. Meanwhile, the water content of fresh porcine muscle is up to 70%, whereas fresh porcine skin only contains 30%.[57] Hence, thiazone is easily extracted when thiazone-PG solution contacts with the free water in muscle. In addition, the dehydration effect of a high concentration of PG contributes to the discharge of water from tissue. Much thiazone crystal are extracted in muscle, whereas no crystals are observed on the skin. With all of the mentioned effects, thiazone is an excellent penetration enhancer for the OC treatment on skin, yet it is not suitable for muscle. Since thiazone mixed with OCAs can easily penetrate through skin and quickly have an effect on subcutaneous muscle tissue, our results demonstrate the inhibition effect of high concentrations of thiazone on the OC of muscle and provide such evidence for the use of thiazone as a penetration enhancer on OC of muscle.

5 Conclusion

Previous studies show that thiazone can remarkably promote the efficiency of OC on skin and is widely used in the transdermal drug delivery. In this paper, we have studied the effect of OC on fresh *in vitro* porcine skin and muscle with the application of different concentrations of the thiazone PG solution. The results of skin experiments suggest that OCA, mixed with thiazone, can sharply improve the effect of OC on porcine skin and thiazone is a good penetration enhancer to skin. These results agree well with other research reports.[33,43,44,46] Interestingly, the effect of thiazone on OC of *in vitro* porcine muscle is absolutely the opposite. With the treatment of thiazone PG solution, crystals of thiazone in muscle are observed and decrease the OC efficiency by an increase in the scattering coefficient of the muscle. Moreover, high-concentration thiazone even inhibits the effect of OC. Hence, our experimental results of thiazone provide valuable evidence for the choices of penetration enhancer during OC studies on muscle. Considering the rapid development of the imaging technique and OCAs such as clarity,[58] scale,[59] see DB,[60] and so on, we expect to be able to expand this work by combining these OCAs with respect to skin, muscle, and neuroimaging. This work may remind researchers that the ancient methods, including the integrating sphere technique, can still play an important role in evaluating the OC efficiency of OCAs with the rapid demand for biological imaging area.

Acknowledgments

The authors would like to thank the Chinese National Key Basic Research Special Fund (Grant No. 2011CB922003), the Natural Science Foundation of China (Grant Nos. 61475078 and 61405097), the Science and Technology Program of Tianjin (Grant Nos. 15JCQNJC02300 and 15JCQNJC02600), the International Science and Technology Cooperation Program of China (Grant No. 2013DFA51430), and the Social Welfare Project of the Ministry of Environmental Protection (Grant No. 201309010). The authors have no conflicts of interest to disclose.

References

1. S. L. Jacques, "Origins of tissue optical properties in the UVA, visible, and NIR regions," *Adv. Opt. Imaging Photon Migr.* **2**, 364–371 (1996).
2. V. V. Tuchin, "Laser light scattering in biomedical diagnostics and therapy," *J. Laser Appl.* **5**, 43–60 (1993).
3. L Oliveira et al., "Optical clearing mechanisms characterization in muscle," *J. Innovative Opt. Health. Sci.* **9**(5), 1650035 (2016).
4. V. V. Tuchin et al., "Light propagation in tissues with controlled optical properties," *J. Biomed. Opt.* **2**, 401–417 (1997).
5. G. Vargas, E. K. Chan, and J. K. Barton, "Use of an agent to reduce scatting in skin," *Lasers Surg. Med.* **24**, 133–141 (1999).
6. G. Vargas, J. K. Barton, and A. J. Welch, "Use of hyperosmotic chemical agent to improve the laser treatment of cutaneous vascular lesions," *J. Biomed. Opt.* **13**(2), 021114 (2008).
7. L. Oliveira et al., "Rat muscle opacity decrease due to the osmosis of a simple mixture," *J. Biomed. Opt.* **15**, 055004 (2010).
8. X. Wen et al., "*In vivo* skin optical clearing by glycerol solutions: mechanism," *J. Biophotonics* **3**(1–2), 44–52 (2010).
9. X. Q. Xu, Q. H. Zhu, and C. J. Sun, "Assessment of the effects of ultrasound-mediated alcohols on skin optical clearing," *J. Biomed. Opt.* **14**(3), 034042 (2009).

10. E. A. Genina, A. N. Bashkatov, and V. V. Tuchin, "Tissue optical immersion clearing," *Expert Rev. Med. Device* **7**(6), 825–842 (2010).
11. H. Zheng et al., "Study on the refractive index matching effect of ultrasound on optical clearing of bio-tissues based on the derivative total reflection method," *Biomed. Opt. Express* **5**(10), 3482–3493 (2014).
12. L. Oliveira et al., "Optical measurements of rat muscle samples under treatment with ethylene glycol and glucose," *J. Innovative Opt. Health Sci.* **6**, 1350012 (2013).
13. L. Oliveira et al., "The characteristic time of glucose diffusion measured for muscle tissue at optical clearing," *Laser Phys.* **23**, 075606 (2013).
14. E. A. Genina, A. N. Bashkatov, and V. V. Tuchin, "Glucose- induced optical clearing effects in tissues and blood," Chapter 21 in *Handbook of Optical Sensing of Glucose in Biological Fluids and Tissues*, V. V. Tuchin, Ed., pp. 657–692, CRC Press, London (2009).
15. X. Guo et al., "In vivo comparison of the optical clearing efficacy of optical clearing agents in human skin by quantifying permeability using optical coherence tomography," *Photochem. Photobiol.* **87**, 734–740 (2011).
16. X. Xu and Q. Zhu, "Feasibility of sonophoretic delivery for effective skin optical clearing," *IEEE Trans. Biomed. Eng.* **55**(4), 1432–1437 (2008).
17. T. T. Yu et al., "Quantitative analysis of dehydration in porcine skin for assessing mechanism of optical clearing," *J. Biomed. Opt.* **16**(9), 095002 (2011).
18. A. Bykov et al., "Imaging of subchondral bone by optical coherence tomography upon optical clearing of articular cartilage," *J. Biophotonics* **9**(3), 270–275 (2016).
19. S. G. Proskurin and I. V. Meglinski, "Optical coherence tomography imaging depth enhancement by superficial skin optical clearing," *Laser Phys. Lett.* **4**(11), 824 (2007).
20. G. Hong et al., "Through skull fluorescence imaging of the brain in a new near-infrared window," *Nat. Photonics* **8**, 723–730 (2014).
21. C. G. Rylander et al., "Dehydration mechanism of optical clearing in tissue," *J. Biomed. Opt.* **11**(4), 041117 (2006).
22. V. V. Tuchin, *Tissue Optics: Light Scattering Methods and Instruments for Medical Diagnosis*, 3rd ed., SPIE Press, Bellingham (2015).
23. V. V. Tuchin, *Optical Clearing of Tissues and Blood*, SPIE Press, Bellingham (2006).
24. L. Oliveira et al., "Diffusion characteristics of ethylene glycol in skeletal muscle," *J. Biomed. Opt.* **20**(5), 051019 (2015).
25. S. Plotnikov et al., "Optical clearing for improved contrast in second harmonic generation imaging of skeletal muscle," *Biophys. J.* **90**, 328–339 (2006).
26. B. Choi et al., "Determination of chemical agent optical clearing potential using in vitro human skin," *Lasers Surg. Med.* **36**, 72–75 (2005).
27. X. Wen et al., "Controlling the scattering of intralipid by using optical clearing agents," *Phys. Med. Biol.* **54**, 6917–6930 (2009).
28. J. Hirshburg et al., "Correlation between collagen solubility and skin optical clearing using sugars," *Lasers Surg. Med.* **39**, 140–144 (2007).
29. A. Yeh et al., "Reversible dissociation of collagen in tissues," *J. Invest. Dermatol.* **121**, 1332–1335 (2003).
30. J. Hirshburg et al., "Collagen solubility correlates with skin optical clearing," *J. Biomed. Opt.* **11**, 040501 (2006).
31. V. Hovhannisyan et al., "Elucidation of the mechanisms of optical clearing in collagen tissue with multiphoton imaging," *J. Biomed. Opt.* **18**(4), 046004 (2013).
32. M. Hammer et al., "Optical properties of ocular fundus tissues-an in vitro study using the double-integrating-sphere technique and inverse Monte Carlo simulation," *Phys. Med. Biol.* **40**, 963–978 (1995).
33. D. Zhu et al., "Imaging dermal blood flow through the intact rat skin with an optical clearing method," *J. Biomed. Opt.* **15**(2), 026008 (2010).
34. C. H. Liu et al., "Enhancement of skin optical clearing efficacy using photo-irradiation," *Lasers Surg. Med.* **42**, 132–140 (2010).
35. J. F. Beek et al., "In vitro double-integrating-sphere optical properties of tissues between 630 and 1064 nm," *Phys. Med. Biol.* **42**, 2255–2261 (1997).
36. J. W. Pickering et al., "Double-integrating-sphere system for measuring the optical properties of tissue," *Appl. Opt.* **32**(4), 399–410 (1993).
37. C. P. Zhang et al., "Determination of the refractive index of a bacteriorhodopsin film," *Opt. Lett.* **19**(18), 1409–1411 (1994).
38. Q. W. Song et al., "Modified critical angle method for measuring the refractive index of bio-optical materials and its application to bacteriorhodopsin," *J. Opt. Soc. Am. B* **12**(5), 797–803 (1995).
39. J. Wang et al., "Effect of tissue fluid on accurate determination of the complex refractive index of animal tissue," *J. Biomed. Opt.* **17**(7), 075011 (2012).
40. J. Wang et al., "Study of dynamic pressure-induced refractive index change using derivative total reflection method," *J. Biomed. Opt.* **18**(11), 117005 (2013).
41. A. I. Roman et al., "Mechanical tissue optical clearing technique increases imaging resolution and contrast through ex vivo porcine skin," *Lasers Surg. Med.* **43**, 814–823 (2011).
42. J. Wang et al., "An innovative transparent cranial window based on skull optical clearing," *Laser Phys. Lett.* **9**(6), 469–473 (2012).
43. X. Wen et al., "Enhanced optical clearing of skin in vivo and optical coherence tomography in-depth imaging," *J. Biomed. Opt.* **17**(6), 066022 (2012).
44. H. Q. Zhong et al., "Synergistic effect of ultrasound and thiazone-PEG 400 on human skin optical clearing in vivo," *Photochem. Photobiol.* **86**, 732–737 (2010).
45. X. Xu and Q. Zhu, "Evaluation of skin optical clearing enhancement with azone as a penetration enhancer," *Opt. Commun.* **279**, 223–228 (2007).
46. Z. W. Zhi et al., "Improve optical clearing of skin in vitro with propylene glycol as a penetration enhancer," *J. Innov. Opt. Health. Sci.* **2**(3), 269–278 (2009).
47. Y. Y. Liu et al., "Optical clearing agents improve photoacoustic imaging in the optical diffusive regime," *Opt. Lett.* **38**(20), 4236–4239 (2013).
48. J. Jiang and R. K. Wang, "Comparing the synergistic effects of oleic acid and dimethyl sulfoxide as vehicles for optical clearing of skin tissue in vitro," *Phys. Med. Biol.* **49**, 5283–5294 (2004).
49. R. Samatham, K. G. Phillips, and S. L. Jacques, "Assessment of optical clearing agents using reflectance-mode confocal scanning laser microscopy," *J. Innovative Opt. Health. Sci.* **3**(3), 183–188 (2010).
50. S. Karma et al., "Enhanced fluorescence imaging with DMSO-mediated optical clearing," *J. Innovative Opt. Health. Sci.* **3**(3), 153–158 (2010).
51. B. Chio et al., "Determination of chemical agent optical clearing potential using in vitro human skin," *Lasers Surg. Med.* **36**, 72–75 (2005).
52. X. Xu and R. K. Wang, "Synergistic effect of hyperosmotic agents of dimethyl sulfoxide and glycerol on optical clearing of gastric tissue studied with near infrared spectroscopy," *Phys. Med. Biol.* **49**(3), 457–468 (2004) .
53. L. Z. Xiong, "A new skin penetration promoter:thiazone," *Fine Spec. Chem.* **21**, 9–11 (2004) (in Chinese).
54. Y. Lee and K. Hwang, "Skin thickness of Korean adults," *Surg. Radiol. Anat.* **24**, 183–189 (2002).
55. S. Stefania et al., "Thickness and echogenicity of the skin in children as assessed by 20-MHz ultrasound," *Dermatology* **201**(3), 218–222 (2000).
56. Y.-N. Li, Z.-X. Li, and Y.-H. Lu, "Measure of skin thickness and study of skin sonogram in adult by high-frequency ultrasound," *Chin. J. Med. Imaging Technol.* **24**, 10 (2008) (in Chinese).
57. E. Wierbicki and F. E. Deatherage, "Water content of meats, determination of water-holding capacity of fresh meats," *J. Agric. Food. Chem.* **6**(5), 387–392 (1958).
58. K. Chung et al., "Structural and molecular interrogation of intact biological systems," *Nature* **497**, 332–337 (2013).
59. H. Hama et al., "Scale: a chemical approach for fluorescence imaging and reconstruction of transparent mouse brain," *Nat. Neurosci.* **14**, 1481–1488 (2011).
60. M.-T. Ke, S. Fujimoto, and T. Imai, "SeeDB: a simple and morphology-preserving optical clearing agent for neuronal circuit reconstruction," *Nat. Neurosci.* **16**, 1154–1161 (2013).

Xiaowei Jin completed her bachelor's degree at the School of Physics, Qiqihar University, China, in June 2014. Currently, she is studying for a master's degree at the School of Physics, Nankai University. Her studies cover optical clearing, optical imaging, and clarity.

Zhichao Deng is a PhD student at the Nankai University of Tianjin, China. He graduated from the School of Physics at the same university in 2011. Currently, he is mainly engaged in the research of biomedical photonics. He has 5 years of experience in the study of tissue refractive index.

Jin Wang received her master's degree in biomedical engineering in 2007 and then joined the School of Physics, Nankai University, China. She received her PhD in optics from Nankai University, China, in 2013. Her research interests include optical clearing, refractive index measurement of biotissue, and optical coherence tomography.

Qing Ye received his PhD in optics from Nankai University, China, in 2008, and then joined the School of Physics, Nankai University. Since 2010, he has been an associate professor of optics at Nankai University specializing on optical coherence tomography, optical clearing, and optical property measurement of biotissue.

Jianchun Mei completed his master's degree at the School of Physics, Nankai University, China, in 2010. The same year, he became an engineer and started to work at the Advanced Technology Institute, Nankai University. He is mainly engaged in the research of photoelectric detection and optical instrument design.

Wenyuan Zhou received his master's and doctoral degrees in 1996 and 2002, respectively. From 2003 to 2012, he worked as an associate professor at Nankai University. Since 2012, he has been a professor of optics at Nankai University. His main research is high-sensitive photon detection, photon imaging technology, and application of biological sensors.

Chunping Zhang has been a professor of physics in the Nankai University since 1995. His main research interests are optical properties and applications of photochromic materials and biomedical photonics.

Jianguo Tian received his PhD from Nankai University in 1991 and then started to teach at the same university as an assistant professor. In 1995, he became a professor. Since 2001, he has become a specially appointed professor at Nankai University. He is mainly engaged in condensed matter physics and photonics, involving optical nonlinear mechanism, and application of photoelectric material properties.